distance of the oHp from the interface. Since the TBA^+ ion is larger than the TEA^+ ion, one expects x_d to be larger in the TBA^+ system. Then, if the position of the adsorbed reactant is independent of the nature of the electrolyte (x_a = constant), it follows that the geometrical factor $(x_d - x_a)/x_d$ should increase in the series $TEA^+ < TPA^+ < TBA^+$. Since α_a is larger in the presence of TEA^+, it follows that λ_a is probably also larger. This could be due to a change in the dielectric constant profile in the inner layer with the nature of the predominant counterion at the oHp such that the ratio ϵ_i/ϵ_{ad} is larger in the TEA^+ system than in the TBA^+ system. Of course, λ also depends on the nature of the counterion in a way that reflects both ion size and dielectric constant. Thus, the dependence of α_a on the nature of the counterion is rather complicated. Furthermore, on the basis of capacity data obtained earlier,[27] the dielectric constant profile in the inner layer is expected to change markedly with potential in the region where the kinetic data were obtained. As a result, λ_a is expected to decrease as the electrode potential becomes more negative, the effect being larger for TBA^+ than for TEA^+. This fact may account for the observation that the value of α_a from CTP in the TBA^+ system is smaller than that found from the ionic strength dependence.

In the case of the alkali-metal[15] and alkaline-earth-metal ions,[17] both k_s and α_a increase in the series $TEA^+ < TPA^+ < TBA^+$. The kinetic data for these systems are obtained at very negative potentials where the dielectric properties of the inner layer are controlled predominantly by the large electrical field at the interface, and remain relatively unchanged over the potential region studied. As a result, the parameters λ_a and λ reflect only the effect of the size of the counterion through the distance x_d. Thus, as x_d increases in the series $TEA^+ < TPA^+ < TBA^+$, λ and λ_a, and therefore, k_s and α_a, also increase. In the case of the alkali-metal ions,[16] nonlinear Tafel plots were observed for systems whose kinetics could be studied over a sufficiently wide range. This observation was attributed to a change in the nature of the rate-determining step with electrode potential. For the present system, the rate constant could not be measured over a wide range due to speed of the reaction so that no conclusion can be made regarding potential dependence of the Tafel slope.

In conclusion, the above results support the model for amalgam formation in which ion transfer in the double layer is the rate-controlling step. However, the double layer effects observed are different in some respects to those observed for systems which react at more negative potentials. The mechanism for the reaction could be clarified further if data were obtained for a slower process in which both the forward and reverse reactions could be studied over a wide potential range. Work in this direction is currently in progress.

Acknowledgment. The financial support of the National Science and Engineering Research Council (NSERC) of Canada is gratefully acknowledged.

Registry No. TEAP, 2567-83-1; TPAP, 15780-02-6; TBAP, 1923-70-2; Cd, 7440-43-9; Hg, 7439-97-6.

Intramolecular Coupling in Metal-Free Binuclear Phthalocyanines

Elaine S. Dodsworth, A. B. P. Lever,* Penny Seymour, and C. C. Leznoff

Department of Chemistry, York University, North York (Toronto), Ontario, Canada M3J 1P3
(Received: June 7, 1985)

The electronic absorption and emission spectra of a series of mononuclear and binuclear metal-free phthalocyanine species are reported. The binuclear species are linked through a benzene ring by a bridge of 0, 1, 2, 4, or 5 atoms. The spectroscopic data for the binuclear species are analyzed in terms of exciton coupling between the two halves of the molecule. Intramolecular coupling is seen to depend upon the nature of the bridging link. In some cases a cofacial conformation is possible; this gives rise to characteristic long-lived emission near 750 nm.

Aggregation is a well-known phenomenon in phthalocyanine chemistry.[1-3] Interactions can occur between adjacent phthalocyanine rings both in organic and aqueous phase, resulting in coupling between the electronic states of two, or more, phthalocyanine units. Recently we reported binuclear phthalocyanines[4-6] involving phthalocyanine units linked through a benzene ring by bridges of 5,[4,5] 2, and 4[6] atoms, and we wish to probe the degree of intramolecular aggregation and the extent of electronic coupling between the two halves of the binuclear molecule. Such coupling is of interest, for example, in the context of the design of multielectron redox catalysts for electrocatalytic and photocatalytic processes, and for studies of energy transfer in biological systems.

Some of the binuclear species described here appear capable of closing in a "clamshell"-like fashion and a spectroscopic probe of this possibility is desirable. Of relevance to this communication are species involving two phthalocyanine units linked via a benzene ring (3 or 4 position) (I) in the following fashion.

label	
Pc-Pc(0)	directly linked phthalocyanine rings
O(1)	phthalocyanine rings linked via an oxygen atom
C(2)	phthalocyanine rings linked via $-CH_2-CH_2-$
C(4)	phthalocyanine rings linked via $-(CH_2)_4-$
Cat(4)	phthalocyanine rings linked via *o*-catecholate, Pc-(cat)-Pc
t-BuCat(4)	phthalocyanine rings linked via 4-*tert*-butyl-*o*-catecholate
EtMeO(5)	phthalocyanine rings linked via $-OCH_2C(Me)(Et)CH_2O-$

The number in parentheses is the number of atoms (0-5) in the bridge link. The phthalocyanine units have neopentoxy groups

(1) Sigel, H.; Waldmeier, P.; Prijs, B. *J. Inorg. Nucl. Chem. Lett.* **1971**, *7*, 161. Bernauer, K.; Fallab, S. *Helv. Chim. Acta* **1961**, *54*, 1287. Monahan, A. R.; Brado, J. A.; DeLuca, A. F. *J. Phys. Chem.* **1972**, *76*, 1994. Abkowitz, M.; Monahan, A. R. *J. Chem. Phys.* **1973**, *58*, 2281.

(2) Blagrove, R. J.; Gruen, L. C. *Aust. J. Chem.* **1972**, *25*, 2553. Schelly, Z. A.; Farina, R. D.; Eyring, E. M. *J. Phys. Chem.* **1970**, *74*, 617. Abel, E. W.; Pratt, J. M.; Whelan, E. *J. Chem. Soc., Dalton Trans.* **1976**, 509.

(3) Schelly, Z. A.; Harward, D. J.; Hemmes, P.; Eyring, E. M. *J. Phys. Chem.* **1970**, *74*, 3040. Farina, R. D.; Halko, D. J.; Swinehart, J. H. *J. Phys. Chem.* **1972**, *76*, 2343. Shelepin, I. V.; Ushakov, O. A.; Gavrilov, V. I. *Elektrokhimiya* **1984**, *20*, 343.

(4) Leznoff, C. C.; Greenberg, S.; Marcuccio, S. M.; Minor, P. C.; Seymour, P.; Lever, A. B. P.; Tomer, K. B. *Inorg. Chim. Acta* **1984**, *89*, L35.

(5) Leznoff, C. C.; Marcuccio, S. M.; Greenberg, S.; Lever, A. B. P.; Tomer, K. B. *Can. J. Chem.* **1985**, *63*, 623.

(6) Marcuccio, S. M.; Svirskaya, P. I.; Greenberg, S.; Lever, A. B. P.; Leznoff, C. C.; Tomer, K. B. *Can. J. Chem.*, in press; manuscripts in preparation.

0022-3654/85/2089-5698$01.50/0

substituted onto each of the three remaining unlinked benzene rings, conferring relatively high solubility in organic solvents. The neopentoxy groups randomly distribute in the 3 or 4 positions. The presence of these isomers (which are very difficult to separate) precludes formation of good crystals and hence X-ray analysis of these systems.

These species may exist in various conformations. Some, e.g., EtMeO(5), may exist in a cofacial or closed "clamshell" configuration and may be thought to "open" or "close" by rotation about the bridge.[4] For others, such as Pc-Pc(0), an intramolecular cofacial conformation is obviously impossible.

Coupling between the two halves of the binuclear molecule may occur through mechanisms described below. In this paper the degree of coupling is explored as a function of the nature of the bridge and of temperature.

Clamshell and cofacial porphyrins have been studied extensively.[7-12] There is a major difference between porphyrins and phthalocyanines in that there is significantly greater intensity in the Q band region of the electronic spectra of the latter, relative to the former, and therefore a larger transition moment. Interactions which are indicated by broadening of the Soret region or small shifts in the Q band region, in the porphyrin series, are readily observable as a much more dramatic effect on the Q band region of the phthalocyanines.

Experimental Section

Electronic absorption spectra were recorded with a Perkin Elmer-Hitachi Model 340 microprocessor spectrometer. Emission and excitation spectra were recorded with a Varian SF330 spectrofluorimeter with appropriate filters to eliminate scattered light. Low-temperature absorption and emission spectra utilized a Beckman variable-temperature cell with quartz windows. Emission lifetimes were obtained by using a York University-constructed nitrogen pulsed laser, a PARC Model 162 Boxcar mainframe with ratio card, and Model 165 and 166 gated integrators. The signal was fed to a Hamamatsu R928 photomultiplier (spectroscopic response 185-930 nm) using an appropriate interference filter.

Toluene was Aldrich Gold Label, and ethanol (100%) was distilled from sodium under nitrogen. The various phthalocyanine species were prepared and purified as reported.[4-6]

The solid-state spectra were obtained by grinding a sample and then smearing on a quartz plate. The Nujol mull spectra were obtained by mulling as for an infrared spectrum.

Results and Discussion

The electronic absorption spectrum of a phthalocyanine species can provide a sensitive probe for the presence or absence of coupling between two (or more) phthalocyanine units. In the absence of coupling, the D_{2h} symmetry, metal-free phthalocyanine shows two strong sharp bands in the 650–720-nm region, plus two weaker vibrational components to higher energy of the main absorption.[13] An example of such a spectrum for a mononuclear metal-free phthalocyanine is shown in Figure 1A. Such a mononuclear species generally shows no sign of intermolecular aggregation in common organic solvents at concentrations below 1×10^{-5} M at room temperature. At higher concentrations, however, intermolecular aggregation can occur.[3,14]

The spectroscopic signature of a binuclear phthalocyanine is determined by the extent of coupling. A fully uncoupled species will display an electronic spectrum apparently identical with that of its mononuclear analogue, as Figure 1A, in this case. Coupling may, in general, be expected to occur (i) through space in a closed cofacial clamshell, (ii) through space between two halves of a binuclear molecule in a partially open or fully open conformation, or (iii) via conjugation through an unsaturated bridge.

Further we anticipate that these binuclear species exist in dynamic equilibrium between the various conformations, depending upon the nature of the bridge. In some cases steric effects may provide barriers to free rotation. However a solution at room temperature is likely to contain a selection of species from strongly coupled to uncoupled and the electronic absorption spectrum will be a composite of the absorption spectra of these species.

These binuclear metal-free phthalocyanines show broad and moderately intense absorption in the 610–650-nm region with weaker peaks on a broad background in the 650–720-nm region (Figure 1B–H), the latter corresponding to the mononuclear absorption (Figure 1A). The shift of absorption intensity to higher energy, relative to the mononuclear species, is a direct indication of coupling,[15] and the broadness may reflect the diversity of conformers in solution. Moreover such spectra are observed essentially unchanged down to 5×10^{-7} M, indicating that the coupling is intramolecular in nature.

In view of the dynamic nature of the equilibrium, it is not useful to try and establish an intraphthalocyanine separation. However, it is feasible to use absorption and emission spectra to ascertain an approximate idea of the degree of coupling, and how this varies with temperature and bridging link. Such information is useful to obtain a clearer picture of the physical chemistry of the binuclear species, and hence facilitate design of useful catalysts. Note that there is some solvent dependence in the electronic spectra, usually reflected in variations in relative peak intensities.[16] These effects are not covered here.

(*i*) *Theory of Intraphthalocyanine Coupling—Qualitative.* The intense absorption in the visible region, the Q band, results from the $a_{1u} \rightarrow e_g$, $\pi \rightarrow \pi^*$ transition, generating an orbitally doubly degenerate state, ^1E_u, in metal phthalocyanines of D_{4h} symmetry. In the free base, the symmetry is lowered to D_{2h} and the excited state is split into two components usually termed Q_y and Q_x. These then are the two principal 650–720-nm-region absorptions in the mononuclear species. The two weaker absorptions are vibrational (1–0) overtones of Q_y and Q_x. The accepted coordinate frame requires $E(Q_x) < E(Q_y)$.[16-18a]

The theory of interaction between phthalocyanine and between porphyrin molecules has been discussed in the literature[15,18-23] especially in the context of cofacial diporphyrins and chlorophyll dimers,[7-12,24,25] aggregated porphyrins,[26,27] and oxo-bridged porphyrins,[19] and is generally based on exciton coupling.[19,28,29]

The exciton coupling model is a *state* interaction theory. The

(7) Dolphin, D. H.; Hiom, J.; Paine III, J. B. *Heterocycles* **1981**, *16*, 417.
(8) Kagan, N. E.; Mauzerall, D.; Merrifield, R. B. *J. Am. Chem. Soc.* **1977**, *99*, 5484.
(9) (a) Collman, J. P.; Elliott, C. M.; Halbert, T. R.; Tovrog, B. S. *Proc. Natl. Acad. Sci. U.S.A.* **1977**, *74*, 18. (b) Mailocq, J. C.; Giannotti, C.; Maillard, P.; Momenteau, M. *Chem. Phys. Lett.* **1984**, *112*, 87.
(10) Schwarz, F. P.; Gouterman, M.; Muljiani, Z.; Dolphin, D. H. *Bioinorg. Chem.* **1972**, *2*, 1. Paine III, J. B.; Dolphin, D. H.; Gouterman, M. *Can. J. Chem.* **1978**, *56*, 1712.
(11) Anton, J. A.; Loach, P. A.; Govindjee *Photochem. Photobiol.* **1978**, *28*, 235.
(12) Chang, C. K. *J. Heterocycl. Chem.* **1977**, *14*, 1285; *Adv. Chem. Ser.* **1979**, *173*, 163.
(13) Gouterman, M. *J. Chem. Phys.* **1959**, *30*, 1139.
(14) Minor, P. C.; Lever, A. B. P., manuscript in preparation.
(15) Hush, N. S.; Woolsey, I. S. *Mol. Phys.* **1971**, *21*, 465.
(16) Jerwin, K.; Wasgestian, F. *Spectrochim. Acta, Part A* **1984**, *40A* 159.
(17) Henriksson, A.; Sundbom, M. *Theor. Chim. Acta* **1972**, *27*, 213.
(18) (a) Edwards, L.; Gouterman, M. *J. Mol. Spectrosc.* **1970**, *33*, 292. (b) Assour, J. M.; Harrison, S. E. *J. Am. Chem. Soc.* **1965**, *87*, 251.
(19) Gouterman, M.; Holten, D.; Lieberman, E. *Chem. Phys.* **1977**, *25*, 139.
(20) Wheeler, B. L.; Nagasubramanian, G.; Bard, A. J.; Schechtman, L. A.; Dininny, D. R.; Kenney, M. E. *J. Am. Chem. Soc.* **1984**, *106*, 7404.
(21) Ciliberto, E.; Doris, K. A.; Pietro, W. J.; Reisner, G. M.; Ellis, D. E.; Fragala, I.; Herbstein, F. H.; Ratner, M. A.; Marks, T. J. *J. Am. Chem. Soc.* **1984**, *106*, 7748.
(22) Lever, A. B. P. *Adv. Inorg. Chem. Radiochem.* **1965**, *7*, 27.
(23) Gouterman, M. In "The Porphyrins"; Dolphin, D., Ed.; Academic Press: New York, 1978; Vol. III, p 1.
(24) Haley, L. V.; Koningstein, J. A. *Can. J. Chem.* **1983**, *61*, 14.
(25) Shipman, L. L.; Cotton, T. M.; Norris, J. R.; Katz, J. J. *J. Am. Chem. Soc.* **1976**, *98*, 8222.
(26) White, W. I. In "The Porphyrins"; Dolphin, D., Ed.; Academic Press: New York, 1978; Vol. V, p 303.
(27) Zachariasse, K. A.; Whitten, D. G. *Chem. Phys. Lett.* **1973**, *22*, 527.
(28) Kasha, M.; Rawls, H. R.; El-Bayoumi, M. A. *Pure Appl. Chem.* **1965**, *11*, 371.
(29) Kasha, M. In "Physical Processes in Radiation Biology"; Augenstein, L., Mason, R., Rosenberg, B., Eds.; Academic Press: New York, 1964; p 23.

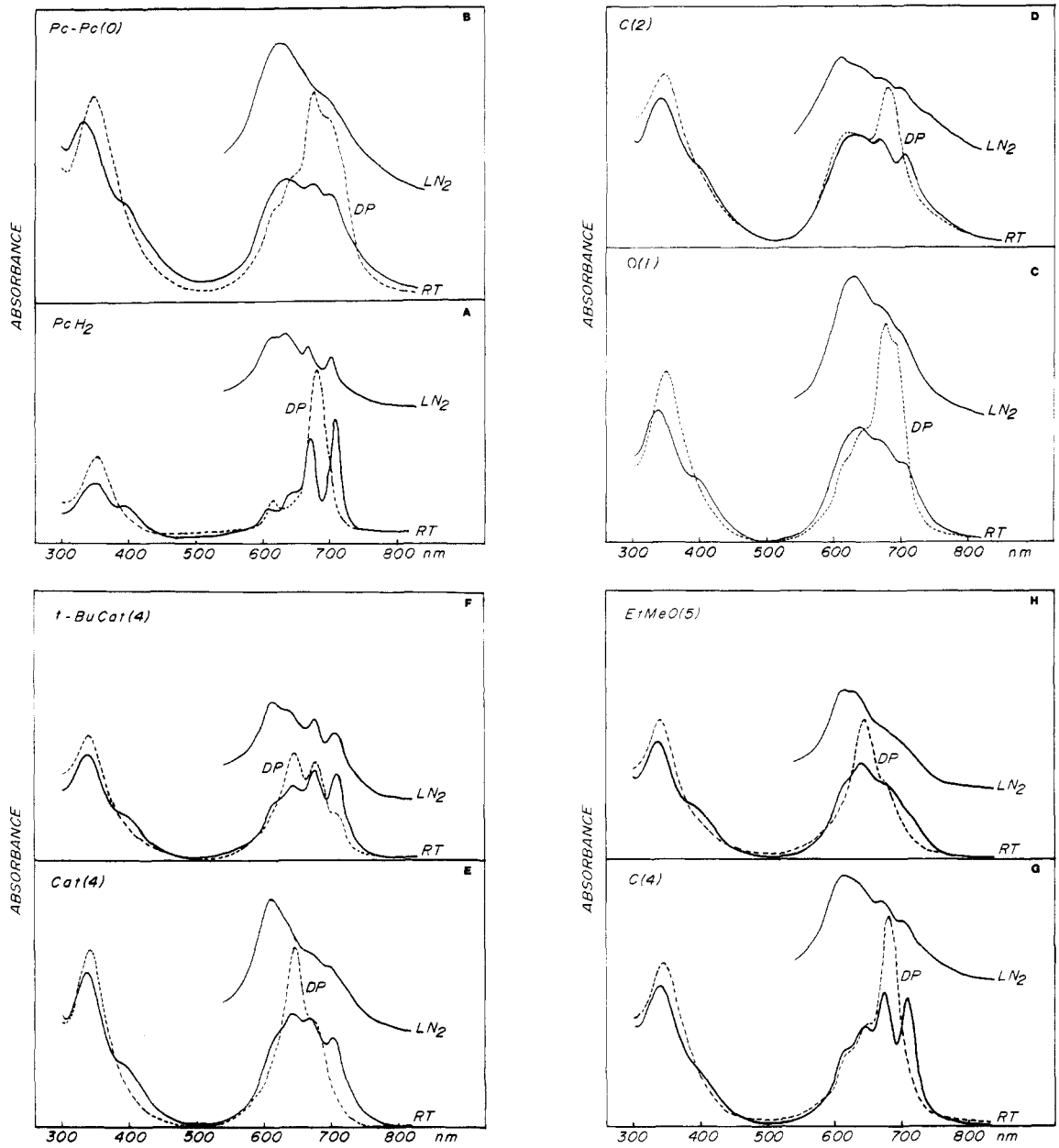

Figure 1. Electronic absorption spectra of mononuclear and binuclear neopentoxyphthalocyanine species as labeled. A, PcH_2; B, Pc-Pc(0); C, O(1); D, C(2); E, Cat(4); F, *t*-BuCat(4); G, C(4); H, EtMeO(5). RT = room temperature in toluene/ethanol (3:2 v/v); LN_2 = liquid nitrogen cooled species in toluene/ethanol (3:2 v/v); DP = deprotonated species obtained by addition of 0.1 mL of TBAOH in methanol to a toluene/ethanol (3 mL, 3:2 v/v) solution, at room temperature. To within the volume change error, the DP and RT spectra are to correct relative scale.

transition moments in the two excited states Q_x, Q_y couple, in- and out-of-phase, between the two halves of the binuclear species. The coupling is proportional to the magnitudes of the transition moments, inversely proportional to the cube of their separation, and has angular dependence. In D_{4h} symmetry, two pairs of doubly degenerate states will then arise, with transitions to the two upper, in-phase coupled states allowed (these will be blue-shifted relative to the mononuclear case), and transitions to the lower out-of-phase combinations being forbidden.[30] In the D_{2h} symmetry of the metal-free derivatives, the Q_x and Q_y states will split and the coupling will result in a pair of nondegenerate in-phase higher energy combinations (Q_{y+},Q_{x+}) and a pair of lower energy out-of-phase combinations (Q_{y-},Q_{x-}) (Figure 2). This theory specifically precludes any overlap between the molecular orbitals of each component. The ground state of the binuclear system corresponds with that of the mononuclear unit but may be stabilized by van der Waals's interaction energy. It is not split.

It is not immediately obvious whether overlap between the two halves of the molecules is likely to be important. With longer bridges and open conformations, overlap can safely be assumed zero. However with the zero bridge system, and especially with the cofacial conformers (see below), overlap could be relevant. Thus, for example, while spectra of binuclear chlorophyll systems have been interpreted in terms of molecular orbital overlap,[24] spectra of stacked silicon phthalocyanines have been interpreted both with[35] and without[15] direct π-overlap.

Orbital overlap is usually described in terms of the "four orbital model" in which the ground-state HOMO and excited-state LUMO on each component of the binuclear species couple in- and out-of-phase. The levels so generated will produce an energy level diagram similar to that shown in Figure 2 but the physical significance is quite different.[24] The molecular orbital model does provide for possible interaction between the HOMO levels of each half of the molecule, resulting in a nondegenerate pair of levels.

In the absence of definitive information concerning orbital overlap in this series of complexes, our discussion will henceforth

(30) The choice of phase is arbitrary depending upon a choice in the phase of the transition moment.[29] One state will be stabilized and one destabilized by the coupling. In the exciton model, the node corresponding to the negative sign is an excitation node, not an electron orbital node. It corresponds with a change in the phase relation between transition moments on each component of the binuclear species.

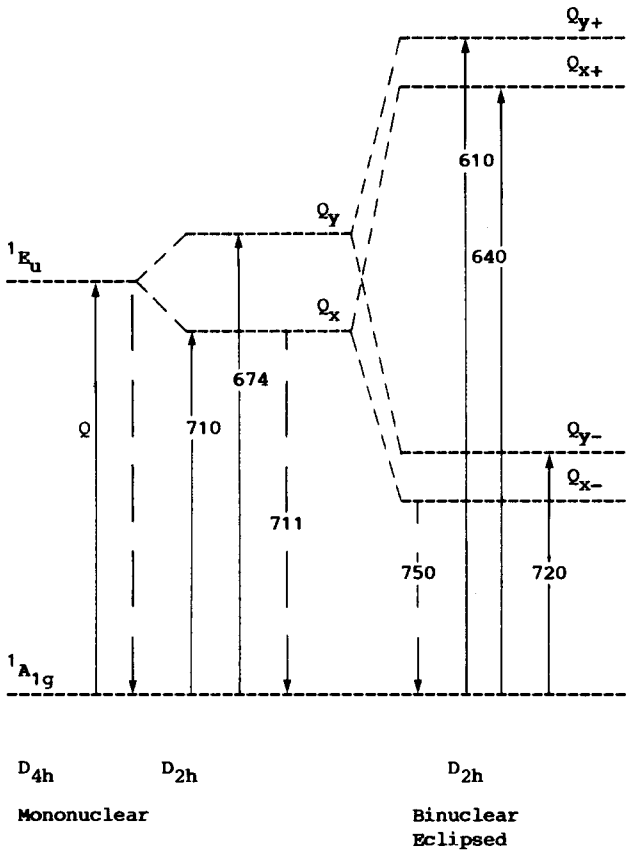

Figure 2. A qualitative orbital energy diagram for exciton coupling. Absorption —, emission - - -. Column 1, a D_{4h} mononuclear metallophthalocyanine species; column 2, a D_{2h} metal-free mononuclear neopentoxyphthalocyanine species; column 3, a D_{2h} binuclear eclipsed neopentoxyphthalocyanine. Typical wavelengths reported in nanometers.

assume the exciton model without orbital overlap.

In the low symmetry of the real binuclear molecules (tilted and slipped conformations etc.), transitions to both the higher and the lower energy combinations (Figure 2) can be expected, yielding intensity both blue- and red-shifted with respect to the mononuclear case.[19] A range of energies is anticipated for the in-phase and out-of-phase combinations, arising from the various conformations. At room temperature a Franck–Condon electronic excitation will see a summation of all the dynamic conformations which exist in solution. Without discussing the added complexities of solvent effects varying from mononuclear to binuclear species, a broad absorption is predicted, shifted to the blue of the mononuclear absorption and possessing a broad weak tail to the red. Superimposed on this envelope will be the two Q peaks of species in which the two halves of the molecule are sufficiently uncoupled to be regarded simply as two independent mononuclear species tied together. This overall appearance is in fact observed for all the binuclear species studied (Figure 1B–H), but with a pair of peaks observed rather prominently to the blue of the mononuclear absorption.

The Soret region (300–450 nm) ($a_{2u} \rightarrow e_g$, $\pi \rightarrow \pi^*$) shows a prominent peak near 350 nm and a well-defined shoulder near 400 nm (Figure 1B–H). This shoulder does not arise from exciton splitting since it is also present in PcH_2 (Figure 1A). However there is a definite blue shift in the Soret peak in the binuclear species compared with the mononuclear.

The intensity of the 650–720-nm peaks relative to those in the 600–650-nm region reflects, qualitatively, the extent of coupling of the binuclear species. This is seen to vary considerably through the series, as discussed below (iii).

(ii) Low-Temperature Absorption Spectra (Toluene/Ethanol). Cooling a solution to a glass at liquid nitrogen temperature causes marked changes in the spectra (Figure 1). In all cases, absorption between 600 and 650 nm becomes more intense relative to absorption in the 650–720-nm region. This is believed to be associated with a greater degree of coupled character at lower temperatures, as previously seen with the cobalt derivatives.[4]

TABLE I: Absorption and Emission Electronic Spectroscopic Data for Mononuclear and Binuclear Metal-Free Phthalocyanine Species in Toluene/Ethanol (3:2 v/v)

		spectra, nm	
species	temp[a]	absorption,[b] (log ε)	emission[c]
PcH_2[d]	RT	347 (4.75), (396) (4.52), 609 (4.43), 645 (4.64), 669 (4.96), 707 (5.03)	709
	LT[e]	340 s, (400) m, (612) s, 634 s, 666 m, 702 m	696, 735 w, 773 w
Pc–Pc(0)	RT	334 (4.90), (390) (4.54), 640 (4.72), 674 (4.71), 700 (4.66)	
	LT	(320) s, (400) s, 625 s	
O(1)	RT	335 (4.97), (390) (4.63), (616) (4.79), 639 (4.84), 669 (4.81), 701 (4.72)	707
	LT	(400) s, 632 s, (668) s, (700) m	699, 730 w, 772 w
C(2)	RT	339 (4.45), (390) (4.29), 621 (4.34), 640 (4.36), 666 (4.38), 705 (4.37)	706
	LT	616 s, 640 s, 667 m, 700 m	698, 734 w, 776 w
C(4)	RT	338 (4.84), (390) (4.48), (620) (4.62), 643 (4.72), 673 (4.77), 708 (4.71)	
	LT	(320) s, (395) s, 614 s, (640) s, 672 s, 700 s	
Cat(4)	RT	338 (5.04), (390) (4.71), (618) (4.89), 640 (4.95), 668 (4.91), 704 (4.80)	706, 780 w
	LT	610 s, (670) w, (700) w	697, *751*
t-BuCat(4)	RT	337 (4.87), (390) (4.52), 620 (4.63), 644 (4.72), 675 (4.79), 710 (4.80)	710, 790 w
	LT	613 s, (640) s, 674 s, 708 m	708, *753*, 780 w
EtMeO(5)	RT	331 (4.93), (390) (4.52), (620) (4.65), 641 (4.72), (673) (4.71), (708) (4.62)	709
	LT	612 s, (636) s, (700) s	700, *763*

[a] RT = room temperature; LT = liquid nitrogen temperature glass. [b] Shoulders in parentheses. [c] For corrected relative intensities, see Table III. All emission peaks, except those shown in italics, originate from the uncoupled conformer of the clamshell or mononuclear species. Italicized peaks originate from cofacially coupled clamshells, see text. [d] Tetraneopentoxyphthalocyanine. [e] Relative intensities of glass spectrum indicated by s = strong, m = medium. w = weak. Absolute intensities are not reliable due to light scattering by glass.

The range of conformations which must exist dynamically in a fluid solution will freeze out, probably to several preferred, and evidently more completely coupled, conformations, at liquid nitrogen temperature. The simplest binuclear species is Pc-Pc(0) whose low-temperature spectrum exhibits more coupled behavior than the room temperature spectrum. It is likely that the two phthalocyanine units rotate around the C–C bond at room temperature but are frozen out at liquid nitrogen temperature, perhaps to a coplanar arrangement, though this may be inhibited by steric interactions between hydrogen atoms on the two linking benzene rings. Entropy considerations should also favor fewer conformations at cryogenic temperatures.[27,31] Intermolecular aggregation is also likely to become more important, and such aggregation may favor a more parallel arrangement of phthalocyanine rings.

The two peaks near 610 and 640 nm vary in their relative intensity in the several binuclear species, probably as a consequence of variations in the preferred low-temperature conformations. However, at this time it is not possible to be more specific.

(iii) Room Temperature Emission Spectra (Toluene/Ethanol). The mononuclear species emits strongly at 709 nm, fluorescing

(31) Turro, N. J. "Modern Molecular Photochemistry"; Benjamin Cummings: Menlo Park, 1979.

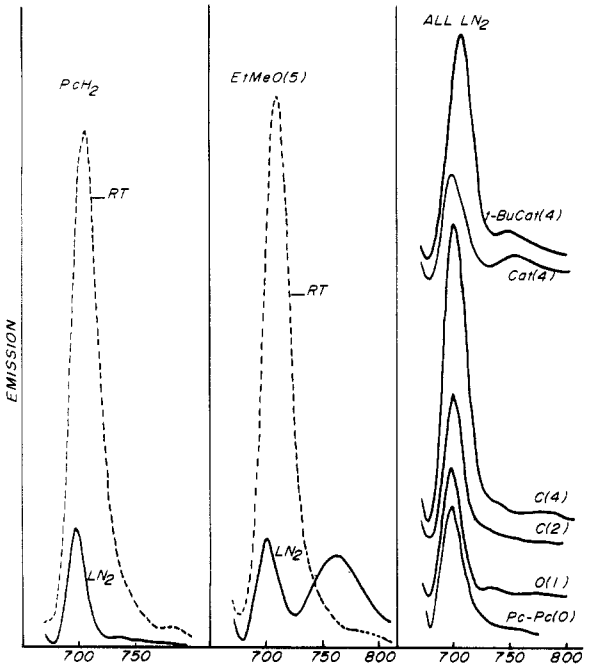

Figure 3. Emission spectra of mononuclear and binuclear metal-free neopentoxyphthalocyanine species in toluene/ethanol (3:2 v/v) solution at room temperature (RT) and at liquid nitrogen temperature (LN_2). Left: Mononuclear neopentoxyphthalocyanine. Middle: The EtMeO(5) species at room temperature and liquid nitrogen temperature. Right: Binuclear species as labeled, at liquid nitrogen temperature. All data were collected at approximately the same concentration, per neopentoxyphthalocyanine unit, with the same instrument settings. Thus the relative intensities will be approximately correct as illustrated.

from the Q band states[18b,23,32,33] with a very small Stokes shift (Figure 3). Much weaker shoulders near 735 and 775 nm are vibrational structure. When a sample is cooled to liquid nitrogen temperature, only weak emission is observed at 696 nm (Figure 3, Table I). The excitation spectra of this 709-nm (or low-temperature 696 nm) feature, or its vibrational satellites, are the same as the absorption spectrum of the mononuclear species, in the Q band region.

The binuclear species also exhibit a band near 710 nm at room temperature in solution, but it is much weaker in emission intensity than in the mononuclear species. Vibrational satellites appear in the same positions as in the mononuclear spectrum. The weaker intensity probably reflects intramolecular self-quenching between the coupled halves of the binuclear species through several possible mechanisms including relaxation to triplet states[29] and nonradiative vibrational relaxation[31] (Figure 3). The excitation spectra of the 710-nm binuclear emission, and its vibrational satellites, are similar to the absorption spectrum of the mononuclear species with maxima between 650 and 720 nm and relatively weaker excitation in the 600–650-nm region (Table II).

The degree of self-quenching may be calculated from the intensity of the ca. 710-nm emission in the binuclear species relative to that of the mononuclear case. These data (Table III) may roughly reflect the degree of uncoupled conformer in each species at room temperature. The extent of coupling decreases in the sequence

$$\text{EtMeO(5)} = \text{C(2)} = \text{Pc-Pc(0)} > \text{O(1)} > \text{C(4)} = \text{Cat(4)} = t\text{-BuCat(4)} > \text{PcH}_2$$

which sequence also approximately parallels the ratio of the peak intensities of the 610–650-nm absorption relative to that at 670–710 nm. This sequence depends, somewhat, upon the nature of the mixture of substituent isomers obtained for each species (see below).

(32) Menzel, E. R.; Rieckhoff, K.; Voigt, E. M. *Chem. Phys. Lett.* **1972**, *13*, 604.
(33) Seybold, P. G.; Gouterman, M. *J. Mol. Spectrosc.* **1969**, *31*, 1.

TABLE II: Excitation Electronic Spectroscopic Data for Mononuclear and Binuclear Metal-Free Phthalocyanine Species in Toluene/Ethanol (3:2 v/v)

species	fluorescent emission,[a] nm	temp	excitation spectra,[a] nm
PcH_2[b]	775[c]	RT	610 w, 642 w, 671 s, 706 s
	736[c]	RT	609 w, 641 w, 671 s, 707 s
	709	RT	612 w, (641), 672 s[d]
	697	LT	607 w, 640 w, 653 vw, 670 s[d]
Pc–Pc(0)	705	RT	(627), (650), 678
	700	LT	615, 648, 679
O(1)	707	RT	614 w, 651 w, 674 s[d]
	699	LT	607 w, 640 w, 652 w, 671 s[d]
	733[c]	LT	608 w, 640 w, 650 w, 671 s, 706 s
	770[c]	LT	614 w, 644 w, 671 s, 704 vs
C(2)	706	RT	613 w, 644 w, 674 s[d]
	698	LT	610 w, 642 w, 672 vs[d]
C(4)	709	RT	614, (650), 676
	700	LT	612, 648, 674
Cat(4)	705	RT	611 w, 640 w, 673 s[d]
	698	LT	610 w, 642 w, 650 vw, 672 s[d]
	754[e]	LT	617 m, 650 m, 674 s, 704 m, 718 s
t-BuCat(4)	710	RT	617 w, 645 w, 676 s[d]
	709	LT	610 w, 650 m, 680 s[d]
	750[e]	LT	620 m, 650 m, 678 s, 718 s
EtMeO(5)	709	RT	613 w, (642), 676 s[d]
	700	LT	610 w, 642 w, 652 w, 672 s[d]
	763[e]	LT	618 m, 653 s, 670 s, 705 s, 720 s

[a] Excitation spectra reported for the fluorescence emission peak as shown. [b] Tetraneopentoxyphthalocyanine. [c] Vibrational satellite of the main ca. 710-nm peak. [d] Excitation peak near 700 nm obscured, too close to emitting line. [e] Cofacial conformation peak. RT = Room temperature; LT = liquid nitrogen temperature.

TABLE III: Relative Emission Intensities of the ca. 700-nm Emission in Mononuclear and Binuclear Metal-Free Phthalocyanine Species in Toluene/Ethanol (3:2 v/v) at Room Temperature[a]

species	rel intensity
PcH_2[b]	100 (8)[c]
O(1)	17 (6.5)
C(4)	33 (3)
t-BuCat(4)	31 (4)
Pc–Pc(0)	12 (3)
C(2)	11 (2.4)
Cat(4)	24 (4)
EtMeO(5)	4 (0.4);[d] 24 (4.8)[d]

[a] The smaller the number, the greater the degree of coupling. Note that scattering prevents an accurate assessment of the liquid nitrogen temperature relative intensities. The data for each species were normalized to the same concentration and corrected for the inner filter effect.[31] The same excitation frequency was used throughout and assumed to remain at constant exciting intensity. [b] Tetraneopentoxyphthalocyanine. [c] Standard deviation in parentheses. [d] Two widely separated chromatographic fractions which must differ significantly in isomer mix.

(iv) Low-Temperature Emission Spectra (Toluene/Ethanol). When cooled to liquid nitrogen temperature, binuclear species show a marked reduction in emission intensity in the 700-nm band, and a shift of about 10 nm to shorter wavelength.

Three binuclear species, EtMeO(5), Cat(4), and *t*-BuCat(4) show an additional emission band near 750 nm which appears in the frozen glass but not in the liquid solution. This emission peak is not observed in the low-temperature glass spectra of the other binuclear species (Figure 3). We propose that the 750-nm emission originates in the coupled conformers. The excitation spectra of the 750-nm band in these three binuclear species also show peaks in the 650–720-nm region but the excitation in the 600–650-nm region is relatively significantly greater than for the 700-nm emission. Moreover there is a pronounced excitation peak near 720 nm which is only weakly evident in the absorption spectrum (Figure 4, Table II). This may be due to direct excitation to an

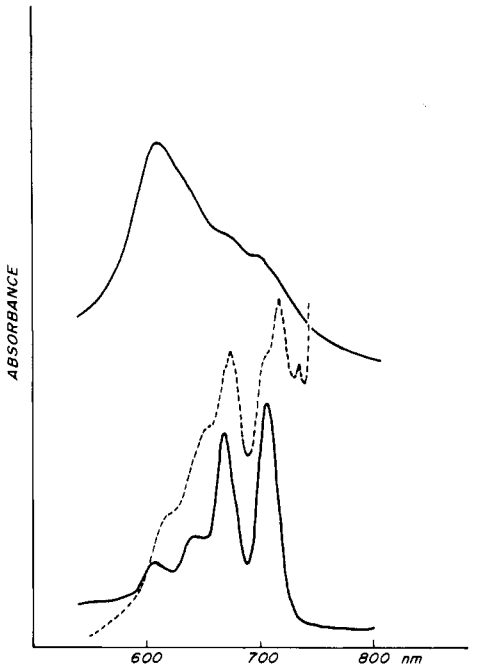

Figure 4. Excitation and related absorption spectra for EtMeO(5). (Upper) EtMeO(5) absorption spectrum in toluene/ethanol glass at 77 K. (Middle) Excitation spectrum of the 750-nm emission (excimer) of EtMeO(5) in toluene/ethanol at 77 K. (Lower) Absorption spectrum of mononuclear PcH_2 in toluene/ethanol (3:2 v/v) at room temperature.

out-of-phase coupled excited state (Q_{y-}) with a high efficiency of relaxation to Q_{x-}.

This behavior parallels, for example, that observed for monomeric and dimeric chlorophyll derivatives, in that the excitation spectra of monomeric and dimeric species are different,[34] and earlier work where excitation spectra discriminated between the origins of emission of dimeric porphyrins[10,11] (see further development below). Certain monomeric zinc porphyrins also show emission from dimeric forms generated in low-temperature solution.[27]

The presence of excitation for the 750-nm emission occurring in the 670–720-nm region, and specifically the peaks therein, implies a mechanism which permits excitation of the uncoupled species to generate emission from the coupled species.[11,34] Energy transfer may be occurring from an excited uncoupled conformer to lower energy states in the coupled species.

(*v*) *Deprotonated Binuclear Metal-Free Phthalocyanine Spectra.* The addition of 0.1–0.2 mL of tetrabutylammonium hydroxide (1 M in MeOH) to solutions (ca. 5×10^{-6} M) of metal-free binuclear species in a cuvette provides a rapid means of obtaining the electronic spectra of the deprotonated species. These are also presented in Figure 1A–H, and Table IV. Deprotonation raises the symmetry of an individual phthalocyanine unit to D_{4h} so that the double Q band should collapse, in the absence of coupling, to a single strong Q band plus its vibrational partner.[23] This is observed for the mononuclear and C(4) species, which show a single peak centered near 680 nm (Figure 1A,G). However the remaining binuclear species show two distinct types of behavior.

In one group we observe a structured Q band centered at 680 nm, obviously a doublet but with closer spacing than the protonated species (Figure 1B,C), while the other group (Figure 1D–F,H) shows prominent absorption near 645 nm, in some cases also associated with 680-nm absorption (Figure 1D,F). As discussed below, these data add considerable insight into the nature of the coupling in these binuclear species.

(*vi*) *Binuclear Conformations.* It is useful to summarize the above data and subdivide the various spectra into groups of observations.

(34) de Wilton, A. C.; Haley, L. V.; Koningstein, J. A. *J. Phys. Chem.* **1984**, *88*, 1077.

TABLE IV: Absorption Electronic Spectroscopic Data for Deprotonated Mononuclear and Binuclear Metal-Free Phthalocyanine Species in Toluene/Ethanol (3:2 v/v)[a]

	absorption spectra (log ε), nm		
species	Soret	Soret half-bandwidth, cm^{-1}	Q band region
Pc^{2-}[b]	352 (4.87)	3900	(614) (4.50), (650) w, 680 (5.12)
Pc–Pc(0)	342 (4.93)	6100	(616) w, (645) (4.73), 675 (4.86), (690) (4.84)
O(1)	340 (5.01)	4750	(610) w, (644) (4.87), 678 (4.92)
C(2)	345 (4.49)	6500	640 (4.37), 679 (4.50)
C(4)	340 (4.89)	5800	(616) w, 646 (4.75), 671 (4.84)
Cat(4)	340 (5.12)	5050	645 (5.12), (670) (4.94), (706) w
t-BuCat(4)	338 (4.92)	5450	(588) w, (612) w, 646 (4.84), 677 (4.81), 710 (4.62)
EtMeO(5)	334 (4.96)	5650	(590) w, 645 (4.80), 677 (4.77)

[a] The deprotonated species were generated in situ, by adding 0.1–0.2 mL of 1 M tetrabutylammonium hydroxide (in methanol) to a solution of the protonated species (ca. 3 mL 5×10^{-6} M). Br = broad, w = weak; data in parentheses are shoulders. [b] Mononuclear.

(a) Only the EtMeO(5), Cat(4), and *t*-BuCat(4) species show the 750-nm emission.

(b) Only the EtMeO(5), Cat(4), and *t*-BuCat(4) deprotonated species show the 645-nm absorption peak as the strongest band.

(c) Only the EtMeO(5), Cat(4), and *t*-BuCat(4) species may exist in a cofacial or approximately cofacial conformation. The others, except perhaps for C(4), are precluded by the configuration of the bridge from becoming cofacial.

(d) Only the mononuclear and C(4) deprotonated species show a single 680-nm absorption.

(e) Only the Pc-Pc(0) and O(1) deprotonated species show a doubled Q band near 680 nm.

(f) The two catechol-bridged deprotonated species show both the 640- and 680-nm absorption.

The existence of 610–650-nm absorption in the O(1) and Pc-Pc(0) binuclear species, and especially the presence of the obviously split Q band in the deprotonated versions of these species, clearly establishes coupling between the halves of these binuclear species, which cannot be cofacial.

The special characteristics of the EtMeO(5), Cat(4), and *t*-BuCat(4) species are most readily explained in terms of *cofacial* intramolecular aggregation, a conclusion supported by construction of molecular models. This is reasonably responsible both for the 750-nm emission and for the shift to 640 nm of the Q band of the deprotonated species. The cofacial conformer could be staggered (D_{4d}) or eclipsed (D_{2h}) subject to steric constraints by the bridge link; they are potentially distinguishable since the former has only one higher energy Q band transition while the latter has two.[19] Both can have electronically allowed lower energy absorption to the Q_{y-},Q_{x-} states. The extreme broadness of the electronic spectra does not permit us to draw any conclusions concerning this question.

Molecular models show that there may be more steric hindrance in the catechol bridged species, than in EtMeO(5). The multiple bands in the spectra of the deprotonated catechol-bridged species may then reflect an equilibrium between cofacial and noncofacial conformations.

Note that the deprotonated species exhibiting 645-nm absorption must be conformationally different from the other species, otherwise they would show 680-nm absorption. This is most readily reconciled by the cofacial conformation. However it is surprising that two Pc^{2-} units would (intramolecularly) aggregate strongly. It is possible that the 640-nm species is only partially deprotonated with the remaining proton(s) forming a hydrogen bond between the two halves. However, we have been unable to modify the spectrum by addition of further excess base, or by addition of a proton sponge.

The single 680-nm band in the deprotonated mononuclear and C(4) binuclear species reveals that the C(4) species does not form a cofacial conformer to any detectable degree. The C(4) binuclear species also has a room temperature electronic spectrum similar to that of the mononuclear species.

The exciton model shown in Figure 2 is valid for both through-space noncofacial and cofacial coupling. Thus one might question why the 750-nm emission is only seen in the cofacial cases. We note that such emission is only seen weakly and at liquid nitrogen temperature when the cofacial conformation is maximized. It is possible that vibrational/rotational modes associated with the bridge of an open noncofacial, but coupled, species provide a pathway for nonradiative relaxation. This could also be a relaxation mechanism at room temperature for those species which show the 750-nm emission at liquid nitrogen temperature. Further note that the intensity of the 750-nm emission is very low (see Figure 3) there probably being energy transfer to the phthalocyanine spin-triplet state near 1000 nm.[9b,11,28,29,32] The cofacial excited states may also have a contribution from charge-transfer states such as $P_a^-P_b^+ \pm P_a^+P_b^-$ which could provide a mechanism for radiationless decay.

It may be useful to view the emission in terms of the formation of an excimer. It is likely that the two halves of the cofacial conformer are more strongly bound in the excited state than in the ground state. Assuming the ground state is much less strongly bound, the emission should be red-shifted from the monomer emission and should be broad and structureless[31] as is the case.

(vii) Quantitative Aspects of Exciton Coupling. In the mononuclear control molecules the intense emission at ca. 14 100 cm^{-1} (709 nm) corresponds to fluorescence from Q_x and is a (0′–0″) transition whose (1′–0″) and (2′–0″) satellites are observable (see Table I). The vibrational progression of approximately 750 cm^{-1} corresponds[18b] with an intense and narrow feature in the infrared spectrum at 744.5 cm^{-1}, due to an aromatic C–H out-of-plane deformation. In the centrosymmetric molecules, the vibrational emission must be g–g and therefore cannot be identified directly with an observed infrared absorption band. However, the ring substituents may weaken this selection rule.

From Figures 1 and 2, the two peaks near 16 350 (610 nm) and 15 625 cm^{-1} (640 nm) in the binuclear derivatives are then the transitions to Q_{y+} and Q_{x+}, respectively. Their separation is almost exactly the same as in the mononuclear species (14 925, 14 165 cm^{-1}).

The cofacial conformer emission at ca. 13 250 cm^{-1} (750 nm) almost certainly arises through emission from the lowest level, Q_{x-}. Since the Stokes shift is expected to be less than 100 cm^{-1} (cf. mononuclear absorption, 14 165 cm^{-1} and emission, 14 105 cm^{-1}), this 13 250-cm^{-1} emission may be the (0′–0″) transition between Q_{x-} and the ground state. This should be relatively long-lived since, at least in the higher symmetry conformers, emission therefrom is forbidden.[29]

The excitation peak at ca. 13 900 cm^{-1} (720 nm) is most reasonably assigned to a transition to Q_{y-}, which then relaxes to Q_{x-} with a high quantum yield.

With these assignments

$$E(Q_{y+}) - E(Q_{x+}) = \text{ca. } 840 \text{ cm}^{-1}$$

$$E(Q_{y-}) - E(Q_{x-}) = \text{ca. } 645 \text{ cm}^{-1}$$

and two direct estimates of the exciton splitting

$$E(Q_{y+}) - E(Q_{y-}) = \text{ca. } 2450 \text{ cm}^{-1}$$

$$E(Q_{x+}) - E(Q_{x-}) = \text{ca. } 2255 \text{ cm}^{-1}$$

This average value of 2350 cm^{-1} corresponds exactly with a LUMO–LUMO interaction splitting energy of 2300 cm^{-1} calculated for a cofacial PcSi–O–SiPc binuclear species.[35] It is significantly larger than observed in various porphyrin and chlorophyll systems.[19,36]

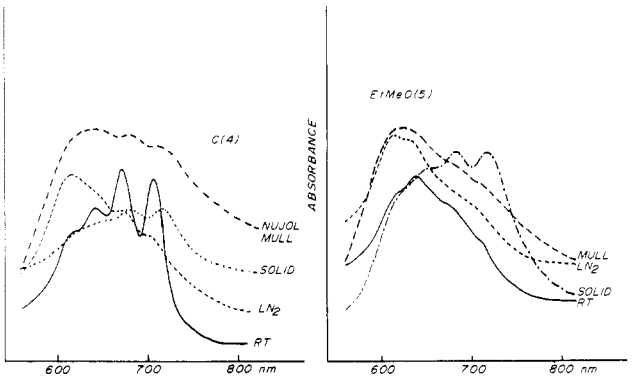

Figure 5. Solid-state crystalline "smear" and Nujol mull spectra of the labeled binuclear species as shown. The toluene/ethanol room temperature and liquid nitrogen glass spectra are repeated to clearly indicate the shifts in absorption from solution to solid state.

TABLE V: Absorption Electronic Spectroscopic Data for Mononuclear and Binuclear Metal-Free Phthalocyanine Species in the Solid State (Smear)

species	absorption spectra, nm
PcH_2[a]	640, 672, 708
Pc–Pc(0)	662, 690, 713
O(1)	662, 690, 713
C(2)	(620), 654, 680, 713
C(4)	618, 654, 679, 718
Cat(4)	(620), 647, 680, 712
t-BuCat(4)	(620), 656, 682, 714
EtMeO(5)	(626), 654, 681, 717

[a] Tetraneopentoxyphthalocyanine. Shoulders in parentheses.

One might try to estimate the average cofacial intramolecular distance using the exciton model and the transition moment evaluated from the oscillator strength of the monomer unit.[28] Although this calculation does yield reasonable numbers, it is considered inaccurate when the intramolecular distance is small compared with the molecular dimensions.[15,37]

(viii) Lifetimes. The ca. 710-nm emission is very short-lived, being allowed fluorescence (within lifetime of our laser <15 ns). The ca. 750-nm emission of the low-temperature cofacial samples originates from a "forbidden" excited state and should therefore have a longer lifetime. Measurements with the sample cooled to 77 K reveal a lifetime for EtMeO(5) of ca. 50 ns. This is in keeping with the model developed here.

(ix) Solid-State Absorption Spectra. To gain insight into the conformations which exist in the solid state, the electronic spectra were recorded as Nujol mulls, and as smears on a quartz plate (Figure 5, Table V). There may be problems arising from scattering effects caused by differences in particle size etc. (sample preparation), but it is possible to make some generalizations.

In all cases, the Nujol mull spectra clearly resemble the spectra of the frozen solutions, though in some cases (PcH_2, Pc-Pc(0), O(1), and C(4)) the LT glass spectra appear to show more coupling than the mulls (more intensity to the blue). These substituted phthalocyanines show some degree of solubility in Nujol, so that the mull could be regarded as a very viscous solution rather than a suspension of small particles.

The solid smear spectra of all the binuclear species show absorption red-shifted from that in solution and from that of the mononuclear. Since unsubstituted phthalocyanines show semiconductor behavior in the solid state,[22] the red shift may be due to the generation of band structure in the solid state, due to intermolecular stacking.

(x) Complexities due to the Presence of Isomers. The mononuclear species PcH_2 exists as a mixture of four geometric isomers as a consequence of the distribution of the neopentoxy

(35) Anderson, A. B.; Gordon, T. L.; Kenney, M. E. *J. Am. Chem. Soc.* **1985**, *107*, 192.

(36) de Wilton, A. C.; Koningstein, J. A. *J. Am. Chem. Soc.* **1984**, *106*, 5088.

(37) Murrell, J. N.; Tanaka, J. *Mol. Phys.* **1964**, *7*, 364.

groups. These isomers will all have similar electronic spectra.

This is not quite true for the binuclear species, since the possible conformations of a specific molecule will be influenced by which of the possible 36 geometric isomers is concerned. In the case of EtMeO(5), for example, the cofacial conformer is apparently not formed with equal ease by all geometric isomers. While we have not found it possible to separate these various geometric isomers, chromatography will yield fractions containing varying mixtures of isomers. The electronic absorption and emission spectra reported in this paper are for representative mixtures of isomers. The reader should be aware that their preparation may have a different mixture and give rise to somewhat different spectroscopic characteristics. The differences will be reflected in a different degree of "average" coupling. We expect such differences to be fairly small except perhaps in the case of EtMeO(5) where we have observed rather larger variations from one sample to another. Note finally that there is only one geometric isomer with respect to the bridging link, say 3,3- but that rotation of one phthalocyanine unit about the other will generate a 3,4- conformational isomer. If rotation is hindered, these two conformers may both be present and may have different spectra.

Summary and Conclusions. The EtMeO(5), Cat(4), and *t*-BuCat(4) binuclears show equilibria between cofacial and noncofacial conformations, with the first, at least in some of its isomers, having the highest proportion of cofacial. Pc-Pc(0) and O(1) are quite similar in behavior, with no possibility for intramolecular cofacial arrangements, but showing significant inter-ring coupling. C(4) is largely uncoupled with little tendency to form cofacial conformers, and with a spectrum, under the various conditions, not very different from the mononuclear. This is rather surprising. Molecular models do not show any obvious reasons for this behavior; it would appear sterically possible to form cofacial conformers. The C(2) species has behavior intermediate between C(4) and O(1) as expected.

The electronic spectra of Co(I), Co(II), and Co(III) derivatives of most of these species have been recorded;[38] in general the degree of coupling between the two halves of the metallated species parallels the behavior discussed here. Of considerable importance is the observation of a rough correlation between the degree of electronic coupling between the two halves of the cobalt species, and the ability of the cobalt species to electrocatalytically reduce molecular oxygen. Future studies will extend to iron complexes and will seek to understand the mechanism causing this important correlation.

Acknowledgment. We are indebted to the Natural Sciences and Engineering Research Council (Ottawa) and the Office of Naval Research (Washington) for financial support, to Shafi Greenberg for synthesis of the neopentoxyphthalocyanine species, and to Liu Wei for recording some of the data.

Registry No. PcH_2, 99128-80-0; Pc-Pc(O), 99147-58-7; O(1), 99128-81-1; C(2), 99128-82-2; C(4), 99128-83-3; Cat(4), 99128-84-4; *t*-BuCat(4), 99128-85-5; EtMeO(5), 99128-86-6.

(38) Liu, W.; Nevin, A.; Hempstead, M. R.; Melnik, M. M.; Lever, A. B. P.; Leznoff, C. C., submitted for publication in *Inorg. Chem.*

Pressure- and Temperature-Induced Phase Transitions in Crystalline Tetracene Monitored via Fluorescence Resonances in a Magnetic Field

R. Jankowiak,[†§] H. Bässler,*[†] and A. Kutoglu[‡]

Fachbereich Physikalische Chemie und Fachbereich Geowissenschaften, Philipps-Universität, D-3550 Marburg, FRG *(Received: June 11, 1985)*

The resonance pattern of the fluorescence intensity of crystalline tetracene in a magnetic field has been analyzed to yield information on the molecular motions accompanying the temperature- or pressure-induced phase transition. The hypothesis has been confirmed that formation of low-temperature and high-pressure phases involves a rotation of the molecule at $^1/_2,^1/_2,0$ by 15° about the N axis. In addition, molecules at 0,0,0 and $^1/_2,^1/_2,0$ rotate by −6 and −9°, respectively, about the L axis. Part of the reorientation occurs continuously upon cooling the high-temperature phase and explains the increase of the Davydov splitting.

Introduction

The aim of this work is to gain further insight into the molecular motions accompanying the phase transition in crystalline tetracene (TC). Recall that TC undergoes a transition from a high-temperature (HT) to a low-temperature (LT) phase somewhere below 200 K. The exact value of the transition temperature T_c depends on the experimental procedure the crystal is subjected to.[1-4] Application of hydrostatic pressure can alter the crystal structure as well.[5] A recent X-ray diffraction study[6] established the triclinic structure of the LT phase and yielded its unit cell parameters. It also indicated that the transition occurs randomly within individual crystal domains which are either preexisting or defined by external forces acting nonuniformly on the crystal and establishing locally different thermodynamic conditions. Unfortunately, the number of reflections was insufficient for carrying out a complete structural analysis. To nevertheless gain some idea of the type of molecular motions involved in the transition, the reliability index[6] ("R value") was calculated as a function of molecular position. It suggested a rotation of the face-centered molecule at $^1/_2,^1/_2,0$ approximately by 15° about the N axis which is normal to the molecular plane.

The difficulty connected with the acquisition of a low-temperature diffractogram of TC which is adequate for endeavoring a complete structural analysis prompted us to search for an al-

[†] Fachbereich Physikalische Chemie.
[‡] Fachbereich Geowissenschaften.
[§] Present address: Ames Laboratory, U.S. DOE, Iowa State University, Ames, IA 50011.

(1) Prikhotko, A. F.; Skorobogatko, A. F. *Opt. Spectrosc. (Engl. Transl.)* **1966**, *10*, 33.
(2) Vaubel, G.; Bässler, H. *Mol. Cryst. Liq. Cryst.* **1970**, *12*, 39.
(3) Turlet, J. M.; Philpott, M. R. *J. Chem. Phys.* **1973**, *62*, 4260.
(4) Kolendritskii, D. D.; Kurik, M. V.; Piryatinskii, Yu. P. *Phys. Status Solidi B* **1979**, *91*, 741.
(5) Kalinowski, J.; Jankowiak, R. *Chem. Phys. Lett.* **1978**, *53*, 56.
(6) Sondermann, U.; Kutoglu, A.; Bässler, H. *J. Phys. Chem.* **1985**, *89*, 1735.

0022-3654/85/2089-5705$01.50/0